

Vortex-Hole Duality: A Unified Picture of Weak- and Strong-Coupling Regimes of Bosonic Ladders with Flux

S. Greschner¹ and T. Vekua²

¹*Institut für Theoretische Physik, Leibniz Universität Hannover, 30167 Hannover, Germany*

²*James Franck Institute, The University of Chicago, Chicago, Illinois 60637, USA*

(Received 28 April 2017; published 18 August 2017)

Two-leg bosonic ladders with flux harbor a remarkable vortex-hole duality between the weak-coupling vortex lattice superfluids and strong-coupling charge-density-wave crystals. The strong-coupling crystalline states, which are realized in the vicinity of π flux, are independent of particle statistics, and are related to the incompressible fractional quantum Hall states in the thin-cylinder limit. These fully gapped ground states, away from π flux, develop nonzero chiral (spin) currents. Contact-interacting quantum gases permit exploration of this vortex-hole duality in experiments.

DOI: [10.1103/PhysRevLett.119.073401](https://doi.org/10.1103/PhysRevLett.119.073401)

Dualities encode important nonperturbative information in statistical, condensed matter and high-energy physics, by mapping weak and strong coupling regimes and providing a way for their unified description [1].

A quantum system, depending on conditions, can manifest one of its dual natures profoundly. In a weakly coupled gas or liquid, where positions of particles are not fixed, at sufficiently low temperatures quantum effects set in, and, as a result, Bose particles can develop phase coherence and superfluidity. For strong repulsive interparticle interactions, crystals can form, where each particle is localized to a certain position in space to get as far as possible from the others. Phases of particles, being conjugate variables of densities, fluctuate strongly in crystals. Fluids can develop eddy currents, or vortices when excited. In superfluids with global phase coherence, vortices get topological protection by quantization. Crystals also harbour excitations of topological nature—e.g., point defects such as vacancies (holes).

The purpose of this Letter is to demonstrate a spectacular correspondence between the topological defects of superfluids and crystals, referred in the following as a vortex-hole duality, realized between weak and strong-coupling regimes of bosonic ladders with flux.

Figure 1 shows the microscopic configurations of local particle currents (arrows) and densities (filled circles) of a few dual weak and strong-coupling ground states of bosonic ladders with flux. In the weak-coupling limit the phases of particles are the relevant degrees of freedom, whereas in strong-coupling particle densities they play a dominant role. Vortices are indicated by the letter V in those plaquettes of Fig. 1, where $\int_{\square} \nabla \Theta dl = 2\pi + \phi$, where Θ is local phase and integration is along the boundary l of the plaquette \square . Holes, defects of the local particle density distribution, are localized on rungs, indicated by the letter H . Vortices (elementary loop currents), topological excitations of a weak-coupling regime, repel each other [2] (like same pole magnets) and vortex lattices (VLs) at a commensurate

vortex density ρ_V are dual to hole crystals of charge-density-wave (CDW) states at $\rho_H = \rho_V$ realized in a strong-coupling regime, as we will show. Table I summarizes the weak and strong-coupling duality relations. In the weak coupling regime of bosonic ladders few VL superfluids were observed [3,4] to survive quantum fluctuations on top of the classical Josephson-junction (JJ) limit [5]. A vortex in the classical JJ limit, where the phase at each ladder site has definite value, carries a quantum of a fluxoid and is localized on $\xi_V \sim \sqrt{J/2J_{\perp}}$ plaquettes [2]. Numerical

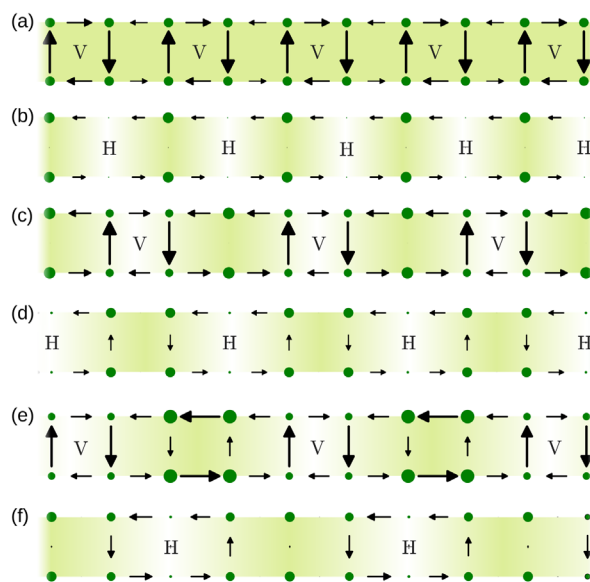


FIG. 1. Microscopic structures of vortex-hole dual configurations of weak (a), (c), (e) and strong-coupling (b), (d), (f) ground states of bosonic ladders with flux. Dual configurations are (a) $\rho_V = 1/2$ vs (b) $\rho_H = 1/2$, (c) $\rho_V = 1/3$ vs (d) $\rho_H = 1/3$, and (e) $\rho_V = 1/4$ vs (f) $\rho_H = 1/4$. Note, that in (a) particle densities are uniform along the ladder, and in (b) particle currents do not show modulations. In contrast, in (c) and (e) particle densities show modulations, similar to particle currents in (d) and (f).

TABLE I. Duality relations between weak and strong-coupling regimes of bosonic ladders with flux. VL states shown in Figs. 1(a), 1(c), and 1(e) survive moderate quantum fluctuations, due to the coherence of the multiboson tunnelings between the ladder legs.

Weak coupling (JJ)	Strong coupling (quantum Hall)
Particle phases, flux	↔ Particle densities, chemical potential
Meissner state	↔ Mott insulator
	Topological excitations
Vortices	↔ Holes
Vortex lattices, ρ_V	↔ Charge density waves, $\rho_H = \rho_V$
	Topological excitations (domain walls)
Fractional fluxoids	↔ Fractional charge
Vortex liquids	↔ Superfluids

simulations of a Bose-Hubbard model on a two-leg ladder with flux showed that particle densities get depleted in the plaquettes where vortices sit, when including quantum fluctuations, and topological excitations of the VL states are domain walls, carrying fractional fluxoids [3,4].

Contact-interacting cold quantum gases loaded in one-dimensional lattices, with an additional second “synthetic” dimension, can explore this duality in the presence of a homogeneous gauge field. The quantum engineering of synthetic orbital magnetism in neutral cold atom optical lattices has achieved tremendous progress during the recent years [6–8]. In particular, the synthetic-dimension approach [9], that combines a one-dimensional optical lattice system with laser assisted transitions between the M internal degrees of freedom which form a compact artificial rung-dimension, allowed for further promising experimental realizations of M -leg ladderlike lattices with an artificial magnetic flux [10–12]. Since all particles on the same synthetic dimensional rung share the same optical lattice site, contact interactions lead to exotic long-ranged interactions along the rungs, which for typical systems [10,11] may be assumed to be $SU(M)$ symmetric. The interplay of long-ranged interactions along the synthetic dimension and homogeneous gauge fields has attracted considerable attention recently, as it gives rise to the ground states bearing analogies with quantum Hall-like behavior [13–21], or exhibiting exotic quantum magnetism [4,18,22–31].

Model.—We consider a two-component, $M = 2$, case and introduce index $\zeta = 0, 1$, running along the synthetic dimension. Our microscopic model is a one-dimensional $SU(2)$ symmetric Bose-Hubbard model with spin-orbit coupling, which is equivalent to spinless bosons on a two-leg ladder with flux and with the same on site interactions as the interactions along the rungs,

$$H = -J \sum_{j=1; \zeta=0,1}^L [b_{j+1, \zeta}^\dagger b_{j, \zeta} + b_{j, \zeta}^\dagger b_{j+1, \zeta}] - \mu \sum_j n_j - J_\perp \sum_j [e^{i\phi_j} b_{j,1}^\dagger b_{j,0} + \text{H.c.}] + \frac{U}{2} \sum_{j, \zeta, \zeta'} n_{j, \zeta} n_{j, \zeta'}. \quad (1)$$

$b_{j, \zeta}$ denotes the bosonic annihilation operator on the ladder site j , ζ , and $n_j = \sum_\zeta n_{j, \zeta}$ denote particle density on rung j . L is the total number of sites along the real space direction, hoppings along ladder legs or rungs are denoted by J/J_\perp , respectively, and U is the Hubbard interaction strength.

We will study model Eq. (1) for $U \gg J, J_\perp$, which is relevant for experiments involving a confinement by a deep optical lattice where the interaction U becomes the dominant energy scale. We consider the limit of $U \rightarrow \infty$, the so-called rung-hard-core limit and address the effects of finite U in the Supplemental Material [32]. Since the exchange of particles is forbidden in the rung-hard-core limit, we need not specify statistics of the particles. Particle density is denoted by $\rho = \sum_j \langle n_j \rangle / L = N/L$. In particular in the rung-hard-core limit the maximal particle density is one particle per ladder rung $\rho = 1$. The density of holes is defined as $\rho_H = 1 - \rho$.

One immediately notices that for a π flux, the spiraling in-plane magnetic field of the model Eq. (1) becomes a staggered field directed along x axes in spin space. Hence, we define an order parameter, corresponding to emergent $U(1)$ symmetry at π flux—the expectation value of $2S^x = \sum_j 2S_j^x = \sum_j b_{j,0}^\dagger b_{j,1} + \text{H.c.}$

CDW states.—Remarkably, as we will show, the staggered field hard-core Hubbard model exhibits a devil-staircaselike structure of CDW phases at fractional fillings $1/2 \leq \rho < 1$. These CDW states are stabilized due to the effective interplay between interactions and the strong magnetic field which tends to localize the particle in tight cyclotron orbitals. At unit filling $\rho = 1$, the ground state is a perfect Néel-Mott insulator state $2\langle S_j^x \rangle = (-1)^j$ [at $U = \infty$, π flux and $\rho = 1$ the Néel-Mott insulator is an exact eigenstate and ground state of model Eq. (1)]. The staggered field induced Néel order at $\phi = \pi$ plays a crucial role in localizing the holes and for emergence of CDW states. This becomes clear if one introduces a single hole on top of the unit filling for $U = \infty$. Then, since particles can not pass each other and since hopping does not flip the spin of the particles, hole motion will scramble the Néel order, by creating a string of displaced particles, which tends to bind the single hole to their initial positions [32].

Nevertheless, one can imagine that two nearest-neighbour holes can move together by forming a bound state, avoiding frustration of the Néel order. The analytic solution of the two-hole problem for the Fermi-Hubbard model shows that two holes when introduced on top of the Néel-Mott state, form bound states (and this happens in fourth order of J) only for $U < U_c$, where $U_c \approx 4J^{2/3}/J_\perp^{2/3}$ for $J_\perp \ll J$ and $U_c = 4\sqrt{6}J_\perp$ for $J_\perp \gg J$ [47]. At $U = \infty$ (where Fermi and Bose-Hubbard models are equivalent), in the ground state holes stay far apart of each other [32], and due to the localized character of single-hole states the CDW phases are formed at rational (commensurate with the lattice) hole densities, exactly in the same way as VL states

are formed in the classical JJ limit [2]: it is a result of the competition between the repulsion among holes (that tries to space holes uniformly apart of each other) and J_{\perp} that binds holes to the rungs.

It is also expected from the above considerations at π flux (especially in the limit of tightly localized on-rung holes $J_{\perp} \gg J$) that the largest hole density for CDW states in the case of contact interactions exhibits a hole on every other rung, the CDW state at $\rho_H = \rho = 1/2$, which is also a fully polarized state. When adding holes on top of the CDW state at $\rho_H = 1/2$, they can move via second order processes $\sim J^2/J_{\perp}$ maintaining the fully polarized background. Hence states for $\rho_H > 1/2$ are expected to be gapless, but showing CDW order with a periodicity of 2 rungs, referred to as supersolid for $J_{\perp} \gg J$ [48]. One can easily obtain the analytical ground state properties of this supersolid ground state for any J_{\perp} in the hard-core limit at π flux. Hence, for $0 < \rho < 1/2$ we obtain for the equation of state $\rho(\mu) = \arccos \{ [(-J_{\perp}^2 + \mu^2)/(2J^2)] - 1 \} / \pi$. The spontaneously developed density imbalance between the even and odd rungs in the supersolid ground state, $\mathcal{O}_{\text{CDW}} = \sum_j (-)^j \langle n_j \rangle / L$, is for any J_{\perp} given by, $\mathcal{O}_{\text{CDW}} = [(J_{\perp}) / (\pi \sqrt{4J^2 + J_{\perp}^2})] \mathcal{F} \{ \pi \rho, [(4J^2)/(4J^2 + J_{\perp}^2)] \}$, $C \mathcal{F}(\phi, k)$. Note, that the CDW order of the supersolid state saturates to a maximal possible value for $J_{\perp}/J \rightarrow \infty$ [48].

For finite $U < \infty$ at $\phi = \pi$, a single hole on top of the unit filling can gain kinetic energy by second-order hopping $\sim J^2/(U + 2J_{\perp})$ without leaving behind a perturbed Néel string; hence, CDW states with $\rho_H \ll 1$ get washed out quickly for $U < \infty$. In addition, with reducing U from the hard-core, particle statistics start to show up and CDW and supersolid states turn out to be more robust for bosons than for fermions [49]. A detailed numerical analysis [32] shows that, for example, the CDW_{2/3} phase remains stable for $U \gtrsim 20J$ for bosons and $U \gtrsim 30J$ for fermions.

Numerics.—In order to obtain a quantitative phase diagram in strong coupling we perform density matrix renormalization group (DMRG) [50,51] calculations of model Eq. (1). For $\rho \geq 1/2$ and $\phi = \pi$, due to strong localization of the holes, infinite DMRG simulations turn out to be very efficient and give the extent and structure of the (largest) CDW phases consistent with the results of finite system size DMRG-simulations [32].

Figure 1 compares dual configurations of local particle densities and currents of weak and strong coupling regimes of bosonic ladders. The microscopic structures of weak-coupling configurations have already been obtained for a single-component Bose-Hubbard model on a two-leg ladder with flux in Ref. [3,4]. Strong-coupling configurations are obtained slightly away from π flux, for model Eq. (1) at $U = \infty$, where one can see that for $\rho_H < 1/2$, local rung and leg currents also show modulations. Exactly at π flux all currents vanish in the strong-coupling limit. However, away from π flux CDW states support nonzero chiral (spin) current.

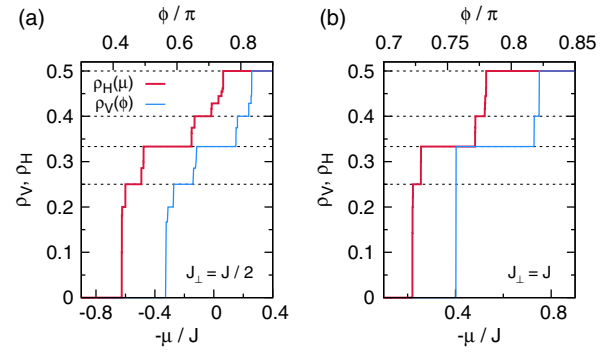


FIG. 2. The dependence of vortex density on flux $\rho_V(\phi)$ in the weak-coupling classical JJ limit and the hole density dependence on chemical potential $\rho_H(\mu)$ in the strong-coupling $U = \infty$, $\phi = \pi$ limit [32] due to vortex-hole duality exhibit a remarkable similarity. With doubling J_{\perp}/J from (a) to (b) fewer plateaus are formed in $\rho_V(\phi)$ and $\rho_H(\mu)$ curves.

In Fig. 2, for different values of J_{\perp}/J , we compare the vortex-density-vs-flux curves, obtained from the phase only model corresponding to the classical JJ limit of the bosonic ladder [32], with the hole-density-vs-chemical-potential curves obtained for model Eq. (1) at $U = \infty$ at π flux.

The phase diagram at π flux for $U = \infty$, in the parameter space of μ/J and J_{\perp}/J , is summarized in Fig. 3. The inset shows $\rho(\mu)$ curves for different values of J_{\perp}/J .

In the weak-coupling picture, including quantum fluctuations (of phases) introduces a mobility of vortices, that can melt VL states into vortex liquids [5]. Analogously, in the strong-coupling limit away from π flux, CDW crystals can melt into superfluids [32]. In Fig. 4 we present the ground state phase diagram as a function of ϕ and ρ for $U = \infty$. Besides Meissner (M-SF) and vortex superfluid (V-SF) phases we observe a Meissner Mott-insulator (spiral MI) phase (which at $\phi = \pi$ evolves into Néel MI) and for $\phi \approx \pi$, the emerging devil's staircaselike set of CDW

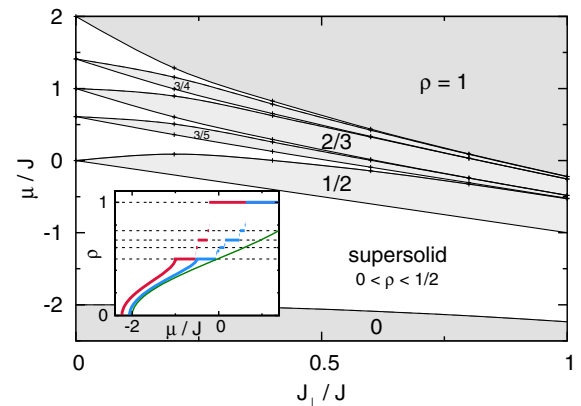


FIG. 3. Ground state phase diagram in the parameter space of μ and J_{\perp} for $U = \infty$ and $\phi = \pi$. For clarity only the most stable fractional CDW phases are shown. Inset shows the equation of state $\rho = \rho(\mu)$ of the $U = \infty$ ladder at π flux for (from left to right) $J_{\perp} = J, J/2$ and 0 .

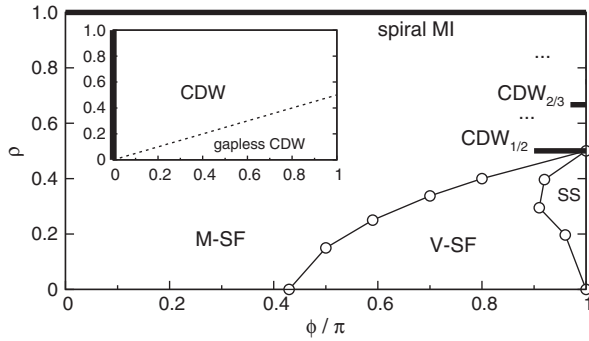


FIG. 4. Ground state phases in parameter space of flux and density for $U = \infty$ and $J_{\perp} = J$. Dots indicate CDW states at rational values of $\rho > 1/2$ at $\phi = \pi$ [53]. Inset shows corresponding phase diagram for $J \ll J_{\perp}$ when number of legs $M \rightarrow \infty$.

phases at fractional fillings and a supersolid (SS) ground state [52].

Relation with quantum Hall states.—In the following we will consider cases corresponding to $M > 2$ and assume that $L \gg M$. We note that the region of stability of the CDW phases may be considerably increased with an increasing number of components M and assuming periodic boundary conditions along the rungs (cylinder or torus geometry). Moreover, following the discussion of Ref. [15], increasing M allows us to relate observed CDW states to fractional quantum Hall states in the thin-cylinder limit. In the case of $M > 2$ -leg cylinder, the Hofstadter-Harper model Eq. (1) is consistently defined for a flux ϕ multiple of $2\pi/M$. We were able to check numerically that at least for $M \leq 6$ at $2\pi/M$ flux, similar picture as described for two-leg ladder at π flux holds. Namely, for low densities, $\rho < (1/M)$, ground states are gapless, with spontaneously formed long-range modulated density, $CDW_{1/M}$. For densities $\rho > (1/M)$ a devil's staircaselike set of CDW states is expected to emerge. For the $U = \infty$ limit, the same arguments can be used to explain this picture as for the two-leg ladders at π flux [32]. This leads us to the limit $M \rightarrow \infty$ to the ground state phase diagram as sketched in the inset of Fig. 4. For particle fillings $\rho < (\phi/2\pi)$ the ground states are gapless and exhibit a CDW order of period $2\pi/\phi$. For larger fillings, $\rho > (\phi/2\pi)$, a region of fully gapped CDW_{ρ} states is formed due to the interplay of commensurate density and periodic potential.

The above discussion allows us to follow the relation between the emerging devil's staircase of fractional CDW phases for the M -leg cylinder at $\phi = 2\pi/M$, realized for $1/M \leq \rho \leq 1$ with the similar incompressible states of a quantum Hall system in the thin-cylinder limit [54–58] realized for the filling $1/M \leq \nu \leq 1$ [32]. Recent works [15–17] indicate that CDW states of M -leg ladders approach corresponding fractional quantum Hall states also in topological properties with increasing M .

Summarizing, we have presented a unifying view of weak and strong-coupling physics of interacting bosons

on two-leg ladders with flux based on vortex-hole duality. This is a broader version of exact duality mappings (such as Kramers-Wannier duality) and implies the equivalence between: the mechanisms of the emergence of VL and CDW states, the ground state degeneracies of the dual configurations, and quantum numbers of topological excitations on top of the dual ground states. All these properties of weak and strong-coupling dual ground states are identical under vortex-hole exchange [59]. Hence, duality can be used as a unifying language for describing weak-coupling and strong-coupling phases of many-body systems, even when there is no exact symmetry mapping between the two, as suggested for two-dimensional systems [60,61]. Once the strongly interacting regime is reached, the predicted vortex-hole duality may be observed within state-of-the-art cold-atom experiments in the near future [32].

We also showed that strong contact interactions give rise to a rich phase diagram for (fermionic as well as bosonic) quantum gases in a one-dimensional lattice, with an additional second synthetic dimension, in the presence of the uniform gauge field. In particular, a devil's staircaselike structure of CDW states emerges at π flux without the need for long-range (e.g., dipolar) interactions between the particles, which can be related to the fractional quantum Hall states in the thin-cylinder limit [15,16,58]. Hence, two cornerstone condensed matter systems (both defined on two-leg ladder lattices)—the classical Josephson-junctions array and the quantum Hall system—can be related to each other through the vortex-hole duality [62].

On the practical side, due to duality, we expect that in the thermodynamic limit a critical value of hopping anisotropy exists in the strong coupling limit J_{\perp}^c/J , like Aubry's breaking-of-analyticity point in the weak-coupling classical JJ limit [64], where the devil's staircase of density vs chemical potential curve changes from incomplete to a complete one. This expectation is consistent with our numerical observation shown in Fig. 2 and in the inset of Fig. 3, where one can see that with increasing J_{\perp}/J less and less densities are realized in the CDW staircase as a function of the chemical potential.

We are grateful to F. Heidrich-Meisner, D. Pirtskhalava, C. Ortix, T. Giamarchi, L. Santos, and P. Wiegmann for useful discussions. S. G. acknowledges the support of the German Research Foundation DFG (Project No. SA 1031/10-1). T. V. was supported in part by the National Science Foundation under the Grant No. NSF DMR-1206648. Simulations were carried out on the cluster system at the Leibniz University of Hannover, Germany.

-
- [1] N. Seiberg, T. Senthil, C. Wang, and E. Witten, *Ann. Phys. (Amsterdam)* **374**, 395 (2016).
[2] M. Kardar, *Phys. Rev. B* **33**, 3125 (1986).

- [3] S. Greschner, M. Piraud, F. Heidrich-Meisner, I. P. McCulloch, U. Schollwöck, and T. Vekua, *Phys. Rev. Lett.* **115**, 190402 (2015).
- [4] S. Greschner, M. Piraud, F. Heidrich-Meisner, I. P. McCulloch, U. Schollwöck, and T. Vekua, *Phys. Rev. A* **94**, 063628 (2016).
- [5] E. Orignac and T. Giamarchi, *Phys. Rev. B* **64**, 144515 (2001).
- [6] M. Aidelsburger, M. Atala, M. Lohse, J. T. Barreiro, B. Paredes, and I. Bloch, *Phys. Rev. Lett.* **111**, 185301 (2013).
- [7] H. Miyake, G. A. Siviloglou, C. J. Kennedy, W. C. Burton, and W. Ketterle, *Phys. Rev. Lett.* **111**, 185302 (2013).
- [8] M. Atala, M. Aidelsburger, M. Lohse, J. T. Barreiro, B. Paredes, and I. Bloch, *Nat. Phys.* **10**, 588 (2014).
- [9] A. Celi, P. Massignan, J. Ruseckas, N. Goldman, I. B. Spielman, G. Juzeliūnas, and M. Lewenstein, *Phys. Rev. Lett.* **112**, 043001 (2014).
- [10] B. K. Stuhl, H.-I. Lu, L. M. Ayccock, D. Genkina, and I. B. Spielman, *Science* **349**, 1514 (2015).
- [11] M. Mancini, G. Pagano, G. Cappellini, L. Livi, M. Rider, J. Catani, C. Sias, P. Zoller, M. Inguscio, M. Dalmonte, and L. Fallani, *Science* **349**, 1510 (2015).
- [12] L. F. Livi, G. Cappellini, M. Diem, L. Franchi, C. Clivati, M. Frittelli, F. Levi, D. Calonico, J. Catani, M. Inguscio, and L. Fallani, *Phys. Rev. Lett.* **117**, 220401 (2016).
- [13] B. N. Narozhny, S. T. Carr, and A. A. Nersesyan, *Phys. Rev. B* **71**, 161101 (2005).
- [14] F. Grusdt and M. Höning, *Phys. Rev. A* **90**, 053623 (2014).
- [15] S. Barbarino, L. Taddia, D. Rossini, L. Mazza, and R. Fazio, *Nat. Commun.* **6**, 8134 (2015).
- [16] T.-S. Zeng, C. Wang, and H. Zhai, *Phys. Rev. Lett.* **115**, 095302 (2015).
- [17] L. Taddia, E. Cornfeld, D. Rossini, L. Mazza, E. Sela, and R. Fazio, *Phys. Rev. Lett.* **118**, 230402 (2017).
- [18] A. Petrescu and K. Le Hur, *Phys. Rev. B* **91**, 054520 (2015).
- [19] E. Cornfeld and E. Sela, *Phys. Rev. B* **92**, 115446 (2015).
- [20] A. Petrescu, M. Piraud, G. Roux, I. McCulloch, and K. L. Hur, [arXiv:1612.05134](https://arxiv.org/abs/1612.05134) [Journal (to be published)].
- [21] M. Calvanese Strinati, E. Cornfeld, D. Rossini, S. Barbarino, M. Dalmonte, R. Fazio, E. Sela, and L. Mazza, *Phys. Rev. X* **7**, 021033 (2017).
- [22] S. K. Ghosh, U. K. Yadav, and V. B. Shenoy, *Phys. Rev. A* **92**, 051602 (2015).
- [23] S. K. Ghosh, S. Greschner, U. K. Yadav, T. Mishra, M. Rizzi, and V. B. Shenoy, *Phys. Rev. A* **95**, 063612 (2017).
- [24] G. Roux, E. Orignac, S. R. White, and D. Poilblanc, *Phys. Rev. B* **76**, 195105 (2007).
- [25] S. T. Carr, B. N. Narozhny, and A. A. Nersesyan, *Phys. Rev. B* **73**, 195114 (2006).
- [26] Z. Yan, S. Wan, and Z. Wang, *Sci. Rep.* **5**, 15927 (2015).
- [27] M. Piraud, F. Heidrich-Meisner, I. P. McCulloch, S. Greschner, T. Vekua, and U. Schollwöck, *Phys. Rev. B* **91**, 140406(R) (2015).
- [28] M. Di Dio, S. De Palo, E. Orignac, R. Citro, and M.-L. Chiofalo, *Phys. Rev. B* **92**, 060506 (2015).
- [29] F. Kolley, M. Piraud, I. McCulloch, U. Schollwöck, and F. Heidrich-Meisner, *New J. Phys.* **17**, 092001 (2015).
- [30] S. Natu, *Phys. Rev. A* **92**, 053623 (2015).
- [31] E. Anisimovas, M. Račiūnas, C. Sträter, A. Eckardt, I. B. Spielman, and G. Juzeliūnas, *Phys. Rev. A* **94**, 063632 (2016).
- [32] See Supplemental Material at <http://link.aps.org/supplemental/10.1103/PhysRevLett.119.073401>, which includes Refs. [33–46], for details on the single-hole localization, numerical methods, the stability of observed ground-state phases for $U < \infty$, and for $\phi < \pi$ as well as an additional discussion on the connection of the two-leg model with the thin-torus limit of fractional quantum Hall effect and a discussion of relevant temperatures and energy scales.
- [33] E. Granato, *Phys. Rev. B* **42**, 4797 (1990).
- [34] J. J. Mazo, F. Falo, and L. M. Floria, *Phys. Rev. B* **52**, 10433 (1995).
- [35] C. Denniston and C. Tang, *Phys. Rev. Lett.* **75**, 3930 (1995).
- [36] R. B. Griffiths and W. Chou, *Phys. Rev. Lett.* **56**, 1929 (1986).
- [37] G. Sun, A. k. Kolezhuk, and T. Vekua, *Phys. Rev. B* **91**, 014418 (2015).
- [38] T. Vekua and G. Sun, *Phys. Rev. B* **94**, 014417 (2016).
- [39] I. Bloch, J. Dalibard, and W. Zwerger, *Rev. Mod. Phys.* **80**, 885 (2008).
- [40] G. Pagano, M. Mancini, G. Cappellini, P. Lombardi, S. Schäfer, H. Hu, X.-J. Liu, J. Catani, C. Sias, M. Inguscio, and L. Fallani, *Nat. Phys.* **10**, 198 (2014).
- [41] M. Höfer, L. Riegger, F. Scazza, C. Hofrichter, D. R. Fernandes, M. M. Parish, J. Levinsen, I. Bloch, and S. Fölling, *Phys. Rev. Lett.* **115**, 265302 (2015).
- [42] R. Zhang, Y. Cheng, H. Zhai, and P. Zhang, *Phys. Rev. Lett.* **115**, 135301 (2015).
- [43] C. Holzhey, F. Larsen, and F. Wilczek, *Nucl. Phys.* **B424**, 443 (1994).
- [44] G. Vidal, J. I. Latorre, E. Rico, and A. Kitaev, *Phys. Rev. Lett.* **90**, 227902 (2003).
- [45] V. E. Korepin, *Phys. Rev. Lett.* **92**, 096402 (2004).
- [46] P. Calabrese and J. J. Cardy, *J. Stat. Mech.* (2004) P06002.
- [47] J. Jaklic and P. Prelovsek, *Phys. Rev. B* **47**, 6142 (1993).
- [48] T. Bilitewski and N. R. Cooper, *Phys. Rev. A* **94**, 023630 (2016).
- [49] The robustness of the supersolid states may be related to the bosonic ferromagnetism.
- [50] S. R. White, *Phys. Rev. Lett.* **69**, 2863 (1992).
- [51] U. Schollwöck, *Ann. Phys. (Amsterdam)* **326**, 96 (2011).
- [52] We note that since the sequence of fractional CDW states and supersolid instability at $\phi = \pi$ are related to $U = \infty$ flat spin-band physics, we do not expect them to be adequately described by the bosonization approach [5].
- [53] Close to the V-SF boundary for $\phi \gtrsim 0.6$ we observe a small region of enhanced density fluctuations which may be connected to the Laughlin-precursor states recently observed for hardcore bosons (without interactions along the rungs) in a similar regime in Ref. [20].
- [54] R. Tao and D. J. Thouless, *Phys. Rev. B* **28**, 1142 (1983).
- [55] A. Seidel, H. Fu, D.-H. Lee, J. M. Leinaas, and J. Moore, *Phys. Rev. Lett.* **95**, 266405 (2005).
- [56] E. J. Bergholtz, T. H. Hansson, M. Hermanns, and A. Karlhede, *Phys. Rev. Lett.* **99**, 256803 (2007).
- [57] P. Rotondo, L. G. Molinari, P. Ratti, and M. Gherardi, *Phys. Rev. Lett.* **116**, 256803 (2016).

- [58] T. Y. Saito and S. Furukawa, *Phys. Rev. A* **95**, 043613 (2017).
- [59] Distinguishing properties of weak-coupling ground states from their dual strong-coupling counterparts is that the former are gapless superfluids, while the latter are gapped crystals.
- [60] R. Fazio and G. Schön, *Phys. Rev. B* **43**, 5307 (1991).
- [61] Y. M. Blanter, R. Fazio, and G. Schön, *Nucl. Phys. B, Proc. Suppl.* **58**, 79 (1997).
- [62] The duality between vortices and charges (bosonic Cooper pairs) across the superfluid-insulator transition has been suggested to be realized in superconducting two-dimensional JJ arrays [60,61,63].
- [63] M. P. Fisher, G. Grinstein, and S. Girvin, *Phys. Rev. Lett.* **64**, 587 (1990).
- [64] S. Aubry, *Lect. Notes Math.* **925**, 221 (1982).